In situ identification strategy of thermoacoustic stability in annular combustors

Driek Rouwenhorst[1], Jakob Hermann[1] and Wolfgang Polifke[2]

Abstract
In annular combustion systems, thermoacoustic eigenmodes can manifest as standing waves, traveling waves or some form in between. Which dynamic solution appears in a combustor depends on details, regarding the flow field and (unintentional) breaking of the cylindrical symmetry of the annular combustion system. When these details are unknown, the specific behavior cannot be predicted from the characteristics of a single burner. Due to the (nearly) degenerate nature of the acoustic solution, annular eigenmodes come in pairs with practically the same eigenfrequency. In order to identify the thermoacoustic modes, conventional analysis of a spectral peak from a measurement does not suffice, because the peak is a superposition of the two eigenmodes. A method has been proposed to identify the two eigenmodes of given azimuthal mode order from multiple simultaneous measurements around the circumference of the combustion system. Using output-only identification on the acoustic signals, it is possible to estimate the individual mode shapes, frequencies and growth rates of the co-existing eigenmode pair. In this work, the strategy is applied to experimental data from an annular combustor. A split in the growth rate pair is observed during stable operation, depending on the equivalence ratio and flame-to-flame distance. It shows that in situ identification of annular thermoacoustics can reveal subtle dynamic effects, which is useful for testing and online monitoring of annular combustors. The moment when instability occurs can be foreseen under prevailing conditions, with simultaneous identification of the azimuthal mode structure.

1. Introduction

In combustion systems with an annular combustion chamber, the low frequency azimuthal modes are a major concern regarding thermoacoustic stability. These modes, in which the flames of individual burners couple with acoustic waves traveling around the combustion chamber circumference, can reach such high amplitudes that a limited operability window must be accepted or structural damage might occur.

Compared to axial thermoacoustic modes, azimuthal modes are more complex. Due to the cylindrical symmetry of the geometry, acoustic solutions consist of pairs with the same wavelength. These degenerate pairs cannot be isolated in frequency domain because their eigenfrequencies are identical. Existing methods to identify modal damping are not suited for the (nearly)

degenerate thermoacoustic mode pairs found in annular combustors.

Another complication is that the flames are excited by transverse acoustics leading to several sources of heat release fluctuations. Following the review paper of O'Connor et al.[1] concerning transverse flame excitation, heat release fluctuations are predominantly generated by axial fluctuations, caused by 'injector coupling'.

[1]IfTA GmbH, Gröbenzell, Germany
[2]Professur für Thermofluiddynamik, Technical University of Munich, Garching, Germany

Corresponding author:
Driek Rouwenhorst, IfTA Ingenieurbuero fuer Thermoakustik GmbH Industriestrasse 33, Groebenzell 82194, Germany.
Email: driek.rouwenhorst@ifta.com

Nevertheless, transverse fluctuations with respect to the flame do influence the heat release directly, for example investigated by Saurabh and Paschereit.[2] These minor contributions to the heat release response can be decisive on the modal behaviour in both the stable and limit cycle regime. With a model including a nonlinear dependency on azimuthal particle velocity, Ghirardo and Juniper[3] were able to obtain standing thermoacoustic limit cycle solutions. A classical stability analysis approach in which axial flame transfer functions (FTFs) are joined to an annular acoustic network is not able to account for a direct transverse flame response.

Several publications on the dynamic behaviour of azimuthal modes in limit cycle have been published, including Worth and Dawson,[4] Noiray and Schuermans[5] and Prieur et al.[6] to name a few. However, limited attention is paid for the fixed-point stable regime. Knowledge about stable operation can be important for optimization and online monitoring of annular combustors in their actual operational state. Rouwenhorst et al.[7] published a strategy to identify the azimuthal eigenmode pairs and obtain their decay rates from real-time measurements. The identification strategy was demonstrated on surrogate data only. The aim of this work is to apply the output-only identification on experimental data from an annular combustor, as a validation of the proposed strategy for practical time series.

The modal amplitudes are a nonlinear or even a discontinuous function of the modal stability, resulting in the step-like amplitude characteristic observed in Figure 2. When the effective damping becomes negative, the amplitude instantaneously rises to dangerous levels in limit cycle. An increase in amplitude before instability is often hard to recognise and a certain amplitude level is not monotonically related to the stability margin. Monitoring of the damping can predict a sudden increase of the amplitude, as it signifies the stability margin. Moreover, the resolution in the stable regime is higher, in comparison to the amplitude of thermoacoustic oscillations.

Several methods are available for the identification of the damping rate of thermoacoustic modes. Noiray[8] proposes to estimate damping or growth rate by the dynamics of the amplitude envelope. In the work of Mejia et al.,[9] four methods are tested on data from a laminar slot burner. However, none of these methods are suited for azimuthal eigenmodes. In general, the methods assume a single mode with no other modes with a nearby eigenfrequency, for example, the fitting of the probability density function. Otherwise, it is assumed the specific eigenmode of interest can be excited, such that the damped oscillating impulse response can be fitted. Azimuthal modes come in

eigenvalue pairs with (nearly) equal eigenfrequencies and decay rates. Moreover, in industrial annular gas turbines, excitation is usually not feasible and it is unknown what azimuthal mode structure will develop. Therefore, the dedicated output-only identification method introduced in Rouwenhorst et al.[7] is proposed for the in situ identification of azimuthal thermoacoustic modes.

2. Methodology

Simultaneously measured acoustic signals recorded around the annular combustion chamber circumference are used to identify the dynamics of azimuthal thermoacoustic modes. The parameters of a low-order model are fitted to the data, such that the key dynamics is captured well. Modal behaviour, growth rates and frequencies can be determined from the model parameters. The objective is to identify the system in the low-amplitude stable regime, which justifies a linear description of the dynamics.

2.1. Model

The slow dynamics of the characteristic waves around the annulus is treated as a pair of coupled harmonic oscillators. The two wave amplitudes F and G are the anticlockwise (ACW) and clockwise (CW) acoustic waves, respectively, with angular resonance frequency ω_a. In combination with corresponding complex harmonic basis functions, they describe the acoustics in the combustion chamber of fixed mode order m.

$$p(t, \theta) = \Re(F e^{i\omega_a t - im\theta} + G e^{i\omega_a t + im\theta}) \qquad (1)$$

It is assumed that the growth rate and frequency modifications that are caused by thermoacoustic feedback are very small compared to the acoustic resonance frequency. This allows linearization around the acoustic solution, decoupling the slow dynamics (amplitude modulations) and the fast dynamics (acoustic oscillations). A system of ordinary differential equations (ODEs) can describe the coupling between the two slowly varying harmonic oscillator amplitudes, including thermoacoustic feedback.

$$\begin{aligned} \frac{dF}{dt} &= a_{FF} F + a_{FG} G \\ \frac{dG}{dt} &= a_{GF} F + a_{GG} G \end{aligned} \qquad (2)$$

Equation (2) governs the azimuthal dynamics of acoustic amplitude similar to the equations used by Noiray et al.,[10] limited to the general linearized form. It describes the rate of change of the amplitudes,

resulting from their own presence, as well as the presence of the wave travelling in the opposite direction. The coefficient a_{FF} comprises the linear heat release response H_F

$$\dot{Q}_F(\theta)e^{-im\theta} = H_F(\theta, \omega_a)Fe^{-im\theta} \quad (3)$$

Through a normalized Rayleigh integral that relates the acoustic growth to the product of the heat release and acoustic pressure distribution in equation (4), the thermoacoustic feedback coefficient a_{FF} (from F to $\dot{F}$) is complete

$$R_{FF} = \frac{1}{\dot{Q}_F}\frac{dF}{dt} \propto \frac{1}{\dot{Q}_F}\int \dot{Q}_F^* e^{im\theta}Fe^{-im\theta}\,\mathrm{d}\theta \quad (4)$$

The * denotes the complex conjugate. Note that the heat release response is evaluated at the acoustic resonance frequency ω_a. By definition of R_{FF}, the feedback coefficient is given by $a_{FF} = H_F R_{FF}$, which can be verified by combining equations (1) to (3). Including a (real-positive) natural acoustic damping coefficient α_F, we have

$$a_{FF} = H_F R_{FF} - \alpha_F \quad (5)$$

Equal definitions for the coefficient a_{FG} read

$$\dot{Q}_G(\theta, \omega_a)e^{im\theta} = H_G(\theta, \omega_a)Ge^{im\theta} \quad (6)$$

$$R_{FG} = \frac{1}{\dot{Q}_G}\frac{dF}{dt} \propto \frac{1}{\dot{Q}_G}\int \dot{Q}_G^* e^{-im\theta}Fe^{-im\theta}\,\mathrm{d}\theta \quad (7)$$

$$a_{FG} = H_G R_{FG} \quad (8)$$

Fundamentally, the cross-coefficient a_{FG} is zero, as the Rayleigh integral vanishes because the acoustic wave and the heat release fluctuations travel in opposite direction, i.e. $\int e^{-2im\theta}\,\mathrm{d}\theta = 0$. However, when H_G is not constant, but has an azimuthal dependency in the form of $H + C_{2m}e^{2m\theta}$, then thermoacoustic coupling between F and G is established, as first identified by Noiray et al.[10]

The two coefficients for the evolution of G are defined in an identical manner.

The dynamic system in equation (2) is subjected to stochastic noise from the turbulent combustion and is measured at several positions around the circumference. In matrix notation, a state-space representation is obtained.

$$\dot{\mathbf{x}} = \mathbf{M}\mathbf{x} + \mathbf{w_x} \quad (9)$$

$$\mathbf{y} = \mathbf{C}\mathbf{x} + \mathbf{w_y} \quad (10)$$

The vector $\mathbf{x} = [F, G]^T$ contains the complex pair of oscillator amplitudes. The complex 2×2 system matrix

$\mathbf{M}$ characterizes the system dynamics with the four coefficients a_{XX}, forced by the stochastic process $\mathbf{w_x}$ which originates from the turbulent combustion. The output vector $\mathbf{y}$ contains the N analytic pressure sensor output signals around the combustor circumference, possibly containing measurement noise $\mathbf{w_y}$. The $N \times 2$ output matrix $\mathbf{C}$ contains information about the angular sensor positions and the monitored mode order. A nomenclature is attached at the end of this paper.

The system matrix $\mathbf{M}$ describes the evolution of the thermoacoustics. Amplitudes remain constant for pure acoustics (undamped and without thermal source term), in which case the system matrix is a null matrix. Damping rates of the two oscillators are real negative values on the diagonal. The anti-diagonal of the matrix establishes linear coupling of the oscillators. The two eigenvalues λ of $\mathbf{M}$ yield the thermoacoustic damping rates and frequency deviations from the acoustic resonance frequency ω_a.

$$\alpha_t = -\Re(\lambda) \quad (11)$$

$$\omega_t = \omega_a + \Im(\lambda) \quad (12)$$

The corresponding eigenvectors provide the mode structures, i.e. whether the observed modes are predominantly standing or traveling waves.

Since the heat release $H_{F/G}$ responds to the waves with their effective thermoacoustic frequency ω_t, rather than the pure acoustic resonance frequency ω_a, the presented model is a linearization of a transcendent eigenvalue problem. In practice, the non-linear behaviour related to a non-constant FTF can lead to a discontinuous solution for continuous parameter changes, as demonstrated in Parmentier et al.[11] A relatively smooth FTF with moderate gain prevents the latter.

In equations (5) and (8), only thermoacoustic feedback and acoustic damping were considered. However, other phenomena could also contribute or influence the matrix coefficients, such as fluid dynamic coupling with the acoustics and an azimuthal flow that convects the acoustic field. In Rouwenhorst et al.,[12] more modelling details can be found. In this work, the system matrix $\mathbf{M}$ is considered as a black box to be identified, ignoring the underlying physical processes.

2.2. System identification

The thermoacoustics as modelled in equation (9) can be identified in several ways, which was shown in Rouwenhorst et al.[7] Such in situ identification yields the coupled thermoacoustic dynamics under the prevailing conditions. The pair of eigenvalues of the system matrix $\mathbf{M}$ yield the eigenfrequency deviations

and damping rates (i.e. stability margin) corresponding to the monitored azimuthal mode order.

In this work, two methods are applied to analyse the experimental data, based on subspace identification and least squares fitting, respectively. Main motivation to apply two methods is cross-validation, because no expected values or analytical predictions for the thermoacoustic system are available.

2.2.1. Preprocessing of the data. In both methods, a bandwidth of the Fourier spectrum is selected, isolating the spectral peak of interest, which is the first azimuthal mode order in this work. Only the positive frequencies in the bandwidth are transferred back to time domain, such that an analytic, filtered signal is obtained. The rectangular filter corresponds to a sinc filter in time domain. This filtering is required to keep oscillating dynamics that is not related to the azimuthal mode pair in question (such as other acoustic modes or blade passing frequencies), out of the analysis. Such dynamics, which is not accounted for in the low-order model description, is a source of structured noise for the identification method. Such noise affects the outcome of the identification significantly more than the (relatively white) noise floor of the measurement, including the quantization error of the pressure data digitization.

Discrete pre-processed data points are available to identify the state-space representation, requiring a discrete formulation of equations (9) and (10) as presented in equations (13) and (14).

$$\mathbf{x}(i + k) = \mathbf{A}\mathbf{x}(i) + \mathbf{v_x}(i) \tag{13}$$

$$\mathbf{y}(i) = \mathbf{C}\mathbf{x}(i) + \mathbf{v_y}(i) \tag{14}$$

In the discrete state-space representation, k is the sample offset between two system states replacing the time derivative in the continuous description. Matrix $\mathbf{A}$ is the discrete version of system matrix $\mathbf{M}$ and the noise vectors $\mathbf{v}$ replace their continuous model parameters $\mathbf{w}$. The eigensolution of the continuous matrix $\mathbf{M}$ is uniquely related to the eigensolution of $\mathbf{A}$.

2.2.2. Stochastic subspace identification. A stochastic subspace identification (SSI) algorithm has been applied following Tanaka and Katayama,[13] in which the entire structure of the discrete state-space representation in equations (13) and (14) is identified. An algorithm, including a weighted singular value decomposition of a matrix with time-delayed data sets, estimates the dominant dynamics for the chosen degrees of freedom. As the mathematics goes beyond the scope of this work, we refer the interested reader to the book of Katayama on this subject.[14]

It is important to note that the mode shape cannot be prescribed in this method, such that it is not possible to enforce a harmonic basis around circumference and exploit knowledge concerning the relation between sensor positions and azimuthal mode order.

Per sensor, three delayed time series were considered with mutual delay intervals of approximately two thermoacoustic cycles. Physically, this means that the dynamics is identified on basis of the evolution of all observed states, during a period of about four cycles each.

2.2.3. Least squares fitting. In the least squares fitting method, we first fit the characteristic waves F and G on basis of the pre-processed sensor outputs, applying the pseudoinverse on equation (14). Subsequently, the discrete system matrix is fitted to the temporal development of a set of these states, by inverting equation (13). Since the state vector is rank two, the two sets of equations in the state space representation can be inverted analytically.

This straightforward fitting strategy is referred to as LSQ. We choose the basis of ACW and CW traveling waves (F and G) to span the eigenspace of acoustic solutions, as used in the model description. For given mode order and at least three measurement locations, the wave amplitudes can now be fitted by taking the Moore–Penrose pseudoinverse of the overdetermined problem in equation (14).

$$\mathbf{x} = (\mathbf{C}^T\mathbf{C})^{-1}\mathbf{C}^T\mathbf{y} \tag{15}$$

When the system states $\mathbf{x}$ are obtained for several consecutive time instances, $\mathbf{A}$ is estimated by inverting equation (13). The concatenation of a set of state vectors $\mathbf{x}$ is denoted by $\mathbf{X}$, yielding the following expression for the pseudoinverse of equation (13).

$$\mathbf{A} = \mathbf{X}_{i+k}\mathbf{X}_i^T(\mathbf{X}_i\mathbf{X}_i^T)^{-1} \tag{16}$$

By using a recursive algorithm to update the estimate of matrix A, the amount of states taken per fit has no influence on the resulting estimate. This allows the real-time tracking of the system's state. Nevertheless, the estimate must be based on data from the past, to average out the forcing noise and measurement noise. Moreover, it must be noted that this two-step identification approach does not yield a bias-free estimate in the presence of measurement noise $\mathbf{v_y}$.

Similarly to SSI, this method identifies the state-space based on a time delay Δt, which is equally set to the span of about four thermoacoustic cycles. A parameter study on the influence of this time delay parameter has shown that it should be picked carefully; after long time delays, the correlation between the two states

vanishes and too short time delays also result in poor results. The latter is thought to be related to the sinc filter used to isolate the frequency peak and/or the temporal correlation of the combustion noise.

3. Experimental data

Data from a laboratory scale annular combustor, kindly provided by Dawson and Worth,[15] have been used to validate the identification strategy on experimental data. The combustor rig, shown in Figure 1 was designed to investigate the azimuthal instabilities, including the effect of burner spacing. Fuel lines transport the perfectly premixed ethylene/air mixture towards the combustion chamber, where swirlers anchor the flames with co-rotating swirl, which is often used in industrial applications. The atmospheric rig is prone to instabilities of the first azimuthal mode order, producing high amplitude limit cycle oscillations with a frequency of around 1700 Hz. The burner spacing was varied by changing the number of fuel lines and swirl burners between the plenum and the annular enclosure, i.e. by replacing the middle section of the combustor in Figure 1.

For equal flame conditions, the Reynolds number at the swirl burners was kept constant in all cases. As a result, the total heat release increases with the number of burners and increasing equivalence ratio, therewith resulting in an increased speed of sound and natural frequencies.

A more extensive description of the experimental setup and measurement methods can be found in the excellent publications of Worth and Dawson.[4,15]

3.1. Measurements

Dynamic pressure was measured in three fuel lines, with $120°$ intervals equally distributed around the combustor circumference. The fuel lines were equipped with two pressure transducers, of which we used the ones closer to the combustion chamber for this work.

Three different burner separation distances were tried, adding up to a respective total of 12, 15 and 18 equally spaced burners around the combustor annulus, to investigate the effect of flame separation distance. For these three cases, a discrete set of 17 equivalence ratios was tested ranging between $\phi = 0.6$ and $\phi = 1$ with steps of 0.025. Measurements were performed under steady operation with a sampling rate of 30 kHz for a period of 4.36 seconds.

The combined root mean square of the three pressure transducers for the three burner separation cases is shown in Figure 2. For every burner spacing, the acoustic amplitude is low for equivalence ratios $\phi \leq 0.8$ and high for equivalence ratios $\phi \geq 0.85$, marking the transition from stable operation to limit cycle operation. The amplitude of the acoustics roughly increases an order of magnitude, corresponding to a factor 100 for the acoustic energy.

With the increasing equivalence ratio, the flame response will change. In first instance, the phase and gain are likely to be altered by the different fuel mixture. In addition, the temperature increase in the combustion chamber should be addressed, which can significantly change the burner impedance, depending on the acoustic characteristics of the plenum and fuel lines.
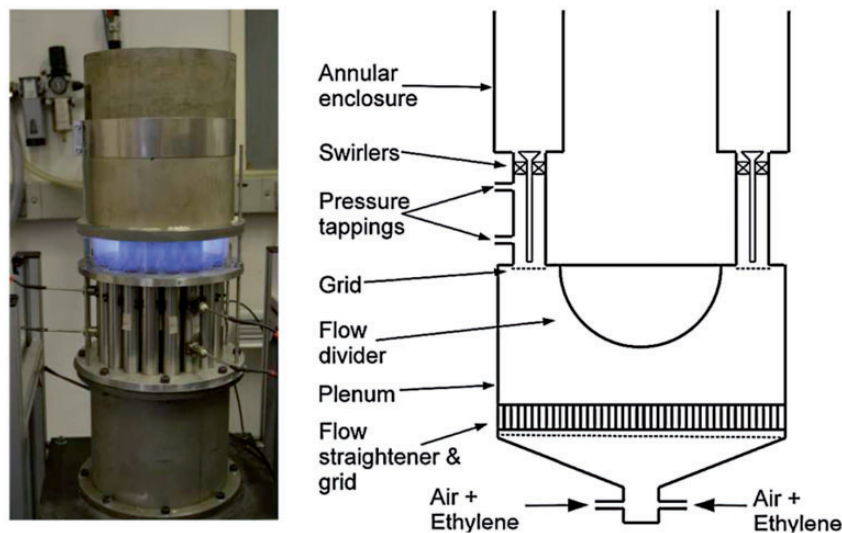
Figure 1. Photo and schematic of the laboratory-scale annular test rig, reproduced from Worth and Dawson[15] with permission.
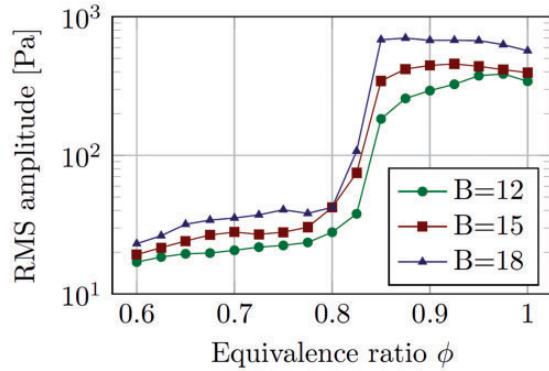
Figure 2. Root mean square of the acoustic amplitude as a function of equivalence ratio and burner spacing, previously published in Worth and Dawson.[4]

Figure 3. Power spectral density (PSD) as a function of equivalence ratio in the analysed bandwidth for the case with 18 burners.

4. Identification results

In this work, the aim is to identify the stability of the system as a whole, rather than discriminating between the phenomena that lead to the instability. The two identification methods are briefly described in Section 2. Methodology is applied to the data to obtain the global characteristics of the system, such as the damping rates and dynamic structure, which are contained in the eigensolution.

A bandwidth $\Delta f = 470$ Hz is used for identification, separating the first azimuthal mode from other spectral content, which moves with the resonance frequency for increasing the equivalence ratio. A waterfall plot with the power spectral density in this bandwidth is shown in Figure 3 for the case of 18 burners. The resonance frequency is located between 1550 and 1800 Hz under all operating conditions. A good isolation of the peaks is required such that other spectral content does not influence the identification process.

Since the operating conditions are kept constant per data set, the entire time series are analysed at once in this work. It must be noted that the same results are obtained using a recursive updating algorithm, generating intermediate identification results after every, for example, 1024th time stamp. Because the entire time series were required to obtain satisfactory stochastic convergence for some cases, intermediate results are not shown and uncertainties could not be evaluated.

A sample delay interval of $k = 1$ is used, such that the time delay is kept small and the correlation between two subsequent states is still clear.

4.1. Damping ratio

The growth rate that is recovered by the real part of the eigenvalue of the system matrix is rewritten to a damping ratio of a harmonic oscillator. To this end, the negated growth rate is divided by the identified
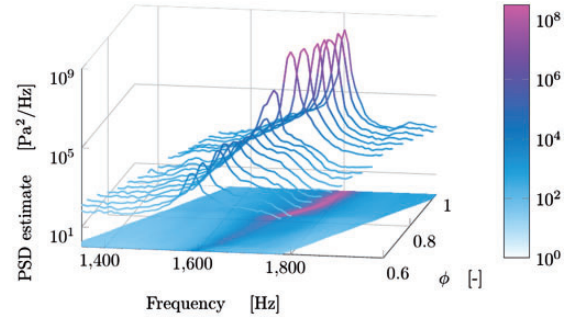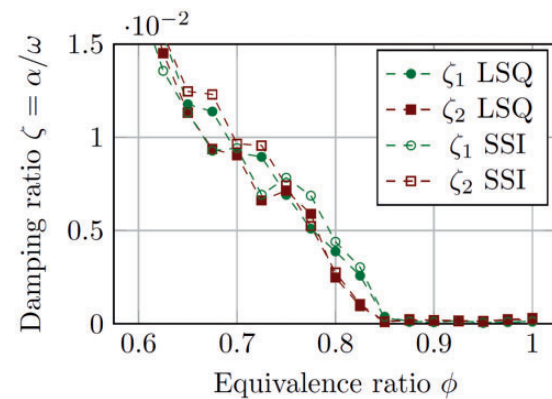
Figure 4. Pair of identified damping ratios as a function of equivalence ratio, for the first azimuthal mode order for the case with 12 burners.

frequency (in radians), which is given by the imaginary part of the eigenvalue.

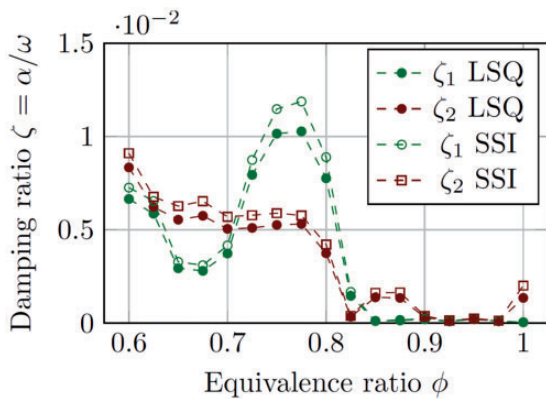$$\zeta_i = \alpha_i/\omega_t = -\Re(\lambda_i)/\omega_t \qquad (17)$$

Figures 4 to 6 show the identified damping ratios for the case with 12, 15 and 18 installed burners, respectively. The results show that the system has a pair of damping ratios at low equivalence ratios, that vanishes between $\phi = 0.8$ and $\phi = 0.85$. The damping ratio does not become negative because the system quickly saturates to a limit cycle, rather than showing continuous exponential growth.

The pair of damping ratios is for many operating conditions clearly distinct, indicating split eigenvalues and a dynamic system that is not (exactly) degenerate. Especially for the case with 18 burners, the stability margins show an interesting behaviour with pronounced splitting of the growth rate.

Even though the effect of eigenvalue splitting is very small in comparison to the resonance frequency,
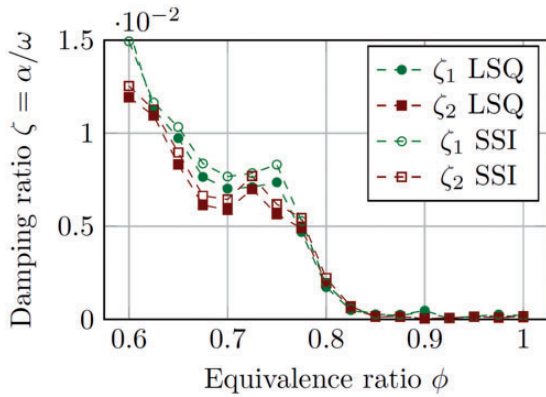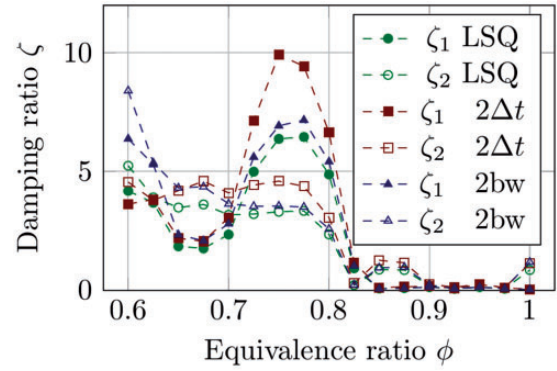
Figure 5. Pair of identified damping ratios as a function of equivalence ratio, for the first azimuthal mode order for the case with 15 burners.

Figure 7. Influence of identification parameters on the identified damping ratios. Longer time delay and wider analysis bandwidth.

Figure 6. Pair of identified damping ratios as a function of equivalence ratio, for the first azimuthal mode order for the case with 18 burners.

it cannot be neglected with respect to the stability margin. This is directly related to the damping ratio, which is typically strongly underdamped ($\zeta \ll 1$) for thermoacoustic eigenmodes.

The near-degenerate pair of fixed-point stable eigenmodes always coexists, being excited by the combustion noise. This stands in contrast to limit cycle oscillations, in which an attractor often has a unique location in the phase space, see for example Noiray et al.[10] Therefore, in limit cycle operation, only one solution is observed (possibly depending on initial conditions), unless the stochastic forcing is quite large with respect to the limit cycle amplitude or the limit cycle itself has a small stability margin. The identification results during limit cycle operation are included in the figures ($\phi \geq 0.85$) and are related to the stability of the limit cycle oscillations. The interpretation and validity of the results for limit cycle oscillations are rather involved and fall outside the scope of this work.

The two methods return remarkably similar results for the identified damping ratios, giving confidence in the implementation of the methods. However, when changing the bandwidth of the identification, or the involved time delays, quite large deviations might occur, especially for the higher damping ratios, that are naturally less pronounced in the data. In Figure 7, the influence of model parameters is visualized for the LSQ method, showing cases with a doubled analysis bandwidth and a doubled time delay. Deviations for the SSI method show a similar trend in the deviations resulting from parameter settings. These deviations can be explained by foreign dynamics in the bandwidth and a loss of correlation between time stamps, respectively. This means that in industrial applications, where the parameters are not tailored for specific operating conditions, the quantitative damping ratio cannot be determined with high accuracy with these methods; nevertheless, a clear qualitative behaviour is revealed.
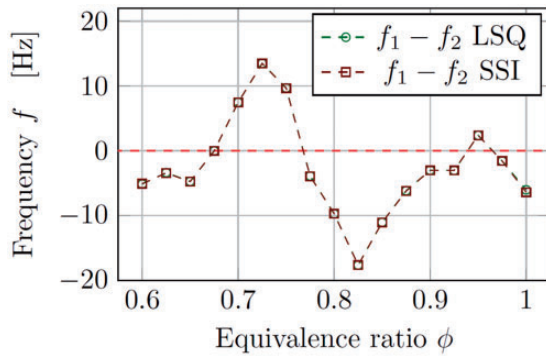
4.2. Eigenvectors

At all distinct operation points, two eigenvalues are obtained by solving the eigenvalue problem of the identified system matrix. The eigenvalues become the subscripts 1 or 2, based on the similarity of the mode structure at adjacent equivalence ratios. So the damping and frequency are ordered, based on the highest resemblance between the eigenvectors, which is given by the maximum of their inner products. This way the connected lines in the plots in Figures 4 to 9 are established, yielding relatively continuous descriptions for the damping ratios and eigenfrequencies as a function of the equivalence ratio.

In Table 1, some eigenvector pairs for the case of 12 and 18 burners are presented in the form of the spin ratio *SR* and the phase difference *Ang* between *F* and *G*.
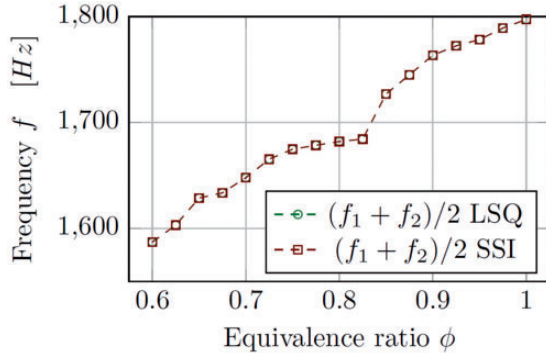
Figure 8. Mean of the identified thermoacoustic eigenfrequency pair as a function of equivalence ratio for 18 burners.

Figure 9. Difference in eigenfrequency of the mode pair as a function of equivalence ratio for 18 burners.

The spin ratio, introduced by Bourgouin et al.,[16] is defined as follows

$$SR = \frac{|F| - |G|}{|F| + |G|} \tag{18}$$

The amplitudes $|F|$ and $|G|$ correspond to the eigenvector contributions of the two waves traveling around the circumference in opposite direction. When they have a similar magnitude ($SR \approx 0$), the mode is a standing wave. In that case, the phase difference between the waves (*Ang*) is of interest, as it determines the angular standing wave orientation. Spin ratios of 1 and −1 refer to pure ACW and CW waves, respectively.

The mode structures (i.e. eigenvectors) are not very coherent, which is attributed to the near-degenerate state of the system and the relatively short measurement duration. Nevertheless, a weak tendency is observed from undefined or predominantly standing wave solutions ($SR < 0.5$) for the case with 12 burners, to predominantly traveling waves ($SR > 0.5$) in the case of 18 burners. Data of more stable operation points are

Table 1. Identified eigenvectors for equivalence ratios shortly before instability, for the distant (12) and close (18) burner separation using LSQ.

Case	ϕ	SR_1	Ang_1	SR_2	Ang_2
12	0.75	0.29	0.49	−0.54	2.02
	0.775	0.01	0.27	−0.78	1.38
	0.8	0.10	−0.29	−0.10	1.83
	0.825	−0.42	−0.35	0.09	1.94
18	0.75	0.81	−1.03	−0.62	−0.33
	0.775	0.78	−1.58	−0.39	−1.77
	0.8	0.82	−0.14	−0.61	−1.88
	0.825	0.70	1.69	−0.47	−1.63

Note: One eigenvector is represented by the spin ratio (SR) and the angle (Ang) between |F| and |G|.

not shown, because the eigenvectors are even less coherent from point to point.

4.3. Eigenfrequencies

In Figure 8, the average of the identified eigen-frequencies (with ω_a added) is shown for the case of 18 burners. With the increasing equivalence ratio, the eigenfrequency rises significantly. This can be expected to play an important role in the stability of the thermoacoustic system.

The splitting of the eigenvalues that caused the distinct damping ratios also causes splitting in the eigenfrequencies, as shown in Figure 9. To the knowledge of the authors, this is the first time a split in azimuthal eigenfrequencies has been discerned from experimental data. The maximum relative deviation $\Delta f/f \approx 0.01$ is of the same order of magnitude as the maximum split in damping ratio.

Based on the eigenvalues splitting at $\phi = 0.825$ in the case of 18 burners, it can be substantiated that fitting of the probability density function would yield an erroneous damping estimation. The frequency split of 18 Hz at very low damping yields a significant thicker peak in the power spectral density. A detailed inspection of the corresponding line of the waterfall plot in Figure 3 (The line near the middle with intermediate amplitude), appears to be composed by two superimposed modal peaks. With higher damping and lower frequency, mode one forms a shoulder on the left side of the peak of mode two. It would yield a significant overestimation of the decay rate, when the peak is designated to a single eigenmode.

The frequency estimates of the two identification methods show a nearly perfect coincidence, such that the SSI-method obscures the marks of the LSQ-method.

4.4. Flame-to-flame distance

The amount of burners has a pronounced effect on the stability, in a non-trivial manner. In the case with the closest flame spacing (18 burners), the damping of one of the eigensolutions varies non-monotonically as a function of the equivalence ratio. On basis of the results, the behaviour cannot be explained in detail, but we will hypothesize a reason for the qualitative behaviour observed.

In the case of 12 burners, the flames barely interact directly. The swirlers cause individual vortices with limited influence of the global flow field. Due to unavoidable minor imperfections in the experimental setup, the cylindrical symmetry is broken, splitting the eigenmodes in two (predominantly) standing wave solutions.

For close burner spacing (18 burners), the flames are merging. This happens in a directional manner, because the swirlers are co-rotating. To get an insight into the complex heat release pattern in this case, please refer to the publication of Worth and Dawson[15] on this topic. One can imagine this can cause an increased flame response to azimuthal particle velocity. Additionally, a global mean flow field develops around the circumference because the vortices on top of the swirlers start to merge, which can lead to eigenfrequency splitting of the acoustic subsystem. These effects can promote traveling wave solutions for the (fixed point stable) azimuthal thermoacoustics.

The case with 15 burners seems to behave in an intermediate state between the system with individual burners and the system with flame–flame interaction.

5. Monitoring strategy

The results show that the proposed identification method can be applied to annular combustors that are prone to azimuthal instabilities. The advantage of the method is that the stability of the mode pair can be identified without prior knowledge about the mode structure. Splitting of the eigenvalues is even detected on a rotationally symmetric laboratory rig in this work. In practice, this can serve as a stability margin that can enhance flexible operation of industrial machines by constant monitoring of potentially hazardous azimuthal eigenmodes.

In particular, the LSQ method is very suited for online determination of the damping, because of the low computational cost of linear regression. For the eigenvalues of the 2×2 system matrix, just a quadratic formula needs to be solved. An updated stability margin is obtained in a fraction of a second after the data were measured, which allows for monitoring, protection and control purposes. The chuck-wise FFT calculation of the raw data is the most computationally expensive step of this method and is usually routinely carried out

already. The SSI method is also feasible to perform in real-time, but does require significantly more DSP processing power.

Such in situ stability determination is beneficial compared to a stability map, in that it reflects the current state of the machine and operation conditions. Effects due to azimuthal velocity and flame-flame interaction are hard to predict, without performing measurements on a full annular setup. Such details are not easily included in a low-order stability analysis, but its effect on the stability can directly be identified, using the in situ state-space representation of the dynamics.

6. Discussion

A very accurate estimation of the decay rate does not necessarily mean it makes an impeccable stability margin. As the case with 18 burners shows, there is no guarantee that the damping decreases monotonically decreases with the control variables at hand. This behaviour needs to be assessed for the specific azimuthal mode for the gas turbine in question, such that a suitable control strategy can be implemented based on the identified damping rate.

In addition, it must be noted that the stability margin (damping ratio) is not necessarily continuous, for continuously changing system parameters, in case that the FTFs change considerably as a function of frequency. In that case, the system matrix depends on its own eigensolution, i.e. the eigensolution is of transcendent nature. Furthermore, triggering can occur due to a nonlinear response of the heat release to the finite acoustic amplitudes. For these reasons, instability might occur before the identified damping reaches zero, which addresses the need for a certain safety margin in practical applications.

7. Conclusions

In previous work,[7] it was shown that azimuthal thermoacoustic dynamics found in annular combustors are effectively described using a complex two-dimensional state-space representation (representing a four-dimensional system). In addition, it was shown that a quantitatively accurate identification of the dynamics can be carried out for surrogate data which is generated on basis of this model description. Assertion that the identification strategy also works successfully on experimental data had not yet been delivered, which is now provided in this work.

The output-only identification strategy has been performed on experimental data of a laboratory scale annular combustor. Qualitatively, the results are promising; consistent damping ratios and modal frequencies are obtained for the rather short experimental data

sets and the pair of damping ratios decrease towards zero before instability occurs and high amplitude limit cycle oscillations are found. The eigenvalue pairs are mostly very similar, yet some structured deviations from a degenerate system are found, which was expected for an experimental setup.

Two different identification methods have been used to obtain the system characteristics of the thermoacoustic dynamics. The results of the two methods are very similar, which gives confidence in the obtained results. However, unlike the artificially generated data, the results depend significantly on model settings, such as analysis bandwidth and the delay parameter. As the actual damping ratios are unknown for these data, it cannot be validated whether the presented damping ratios are quantitatively accurate.

The case with close burner spacing (18 burners) shows predominantly traveling wave solutions, with pronounced splitting of the eigenvalues. Although the physics cannot be explained on basis of the results, the effect it has on both the stability and eigenfrequency splitting is captured in detail. We hypothesize that the flame response to azimuthal acoustic excitation and the mean flow field in the annulus contribute to the eigenvalue splitting.

It is observed that eigenvalue splitting can become relevant for vanishing system stability, even though the magnitude is negligible with respect to the acoustic resonance frequency. This observation stresses the necessity to decompose the signals on a two-dimensional basis, allowing for the typical azimuthal solutions as a mix of traveling and standing waves. In less controlled environments of industrial applications, eigenvalue splitting is expected to be more pronounced.

In the first place, the identification can serve as a stability margin measure to monitor annular combustion systems during operation. When the stability margin falls below a predefined threshold, a signal would be sent to the control system to freeze the current operating conditions, or even to retreat to operating conditions that were further away from the instability.

When the dependency on model parameters is understood better and a validation strategy is developed, identification results can be compared in a quantitative way. In gas turbine testing, the methods can enable quantitative comparison of the thermoacoustic behaviour, when changes or upgrades are made to the machine.

Acknowledgements

Declaration of Conflicting Interests

Funding

References

1. O'Connor J, Acharya V and Lieuwen T. Transverse combustion instabilities: acoustic, fluid mechanic, and flame processes. *Prog Energy Combust Sci* 2015; 49: 1–49.

2. Saurabh A and Paschereit CO. Combustion instabilities in a swirl flow combustor with transverse extensions. In: *ASME turbo expo 2013*: *turbine technical conference and exposition, Vols. 1B*: *combustion, fuels and emissions*, San Antonio, Texas, USA, 3–7 June 2013, p. V01BT04A057. San Antonio: ASME.

3. Ghirardo G and Juniper MP. Azimuthal instabilities in annular combustors: standing and spinning modes. *Proc R Soc A* 2013; 469: 20130232.

4. Worth NA and Dawson JR. Self-excited circumferential instabilities in a model annular gas turbine combustor: global flame dynamics. *Proc Combust Inst* 2013; 34: 3127–3134.

5. Noiray N and Schuermans B. On the dynamic nature of azimuthal thermoacoustic modes in annular gas turbine combustion chamber. *Proc R Soc A* 2013; 469: 20120535.

6. Prieur K, Durox D, Schuller T, et al. A hysteresis phenomenon leading to spinning or standing azimuthal instabilities in an annular combustor. *Combust Flame* 2016; 175: 283–291.

7. Rouwenhorst D, Hermann J and Polifke W. Online monitoring of thermoacoustic eigenmodes in annular combustion systems based on a state-space model. *J Eng Gas Turbines Power* 2016; 139: 021502.

8. Noiray N. Linear growth rate estimation from dynamics and statistics of acoustic signal envelope in turbulent combustors. *J Eng Gas Turbines Power* 2016; 139: 041503.

9. Mejia D, Miguel-Brebion M and Selle L. On the experimental determination of growth and damping rates for. *Combust Flame* 2016; 169: 287–296.

10. Noiray N, Bothien M and Schuermans B. Investigation of azimuthal staging concepts in annular gas turbines. *Combust Theory Modell* 2011; 15: 585–606.

11. Parmentier J-F, Salas P, Wolf P, et al. A simple analytical model to study and control azimuthal instabilities in annular combustion chambers. *Combust Flame* 2012; 159: 2374–2387.

12. Rouwenhorst D, Hermann J and Polifke W. Bifurcation study of azimuthal bulk flow in annular combustion systems with cylindrical symmetry breaking. *Int J Spray Combust Dyn* 2017; 9: 438–451.

13. Tanaka H and Katayama T. Stochastic subspace identification via "LQ decomposition". In: *42nd IEEE conference on decision and control*, Maui, Hawaii, USA, 9–12 December 2003, Vol. 4, pp.3467–72. Maui: IEEE.

14. Katayama T. *Subspace methods for system identification*. London: Springer-Verlag London Limited, 2005.

15. Worth NA and Dawson JR. Modal dynamics of self-excited azimuthal instabilities in an annular combustion chamber. *Combust Flame* 2013; 160: 2476–2489.

16. Bourgouin J, Durox D, Moeck JP, et al. Self-sustained instabilities in an annular combustor coupled by azimuthal and longitudinal acoustic modes. In: *ASME turbo expo 2013: turbine technical conference and exposition. Volume 1B: combustion, fuels and emissions*, San Antonio, Texas, USA, 3–7 June 2013, p. V01BT04A007. San Antonio: ASME.

Appendix

Notation

a	coefficient of matrix M
A	discrete system matrix
Ang	angle between waves F and G
C	output matrix
f	frequency
F	ACW acoustic wave
G	CW acoustic wave
H	Heat release response
m	mode order
M	system matrix
R	Rayleigh integral
SR	Spin ratio
v	discrete noise vector
w	noise vector
x	state vector
X	matrix of concatenated state vectors
y	output vector
α	decay rate
ζ	damping ratio
λ	eigenvalue
ϕ	equivalence ratio
ω_a	acoustic resonance frequency
ω_t	thermoacoustic eigenfrequency
$\Im(.)$	imaginary part
$\Re(.)$	real part